Single-cell transcriptomics reveals granzyme K-expressing cytotoxic Tfh cells in tertiary lymphoid structures in IgG4-RD

青柳, 龍一

Brief report

Single-cell transcriptomics reveals granzyme K–expressing cytotoxic Tfh cells in tertiary lymphoid structures in IgG4-RD

Ryuichi Aoyagi, DDS,[a]* Takashi Maehara, DDS, PhD,[a,b]* Risako Koga, DDS,[a]* Ryusuke Munemura, DDS,[a] Tadashi Tomonaga, DDS,[a] Yuka Murakami, DDS,[a] Atsushi Doi, PhD,[c] Hidetaka Yamamoto, MD, PhD,[d] Tamotsu Kiyoshima, DDS, PhD,[e] Shintaro Kawano, DDS, PhD,[a] and Seiji Nakamura, DDS, PhD[a] *Fukuoka and Okayama, Japan*

GRAPHICAL ABSTRACT

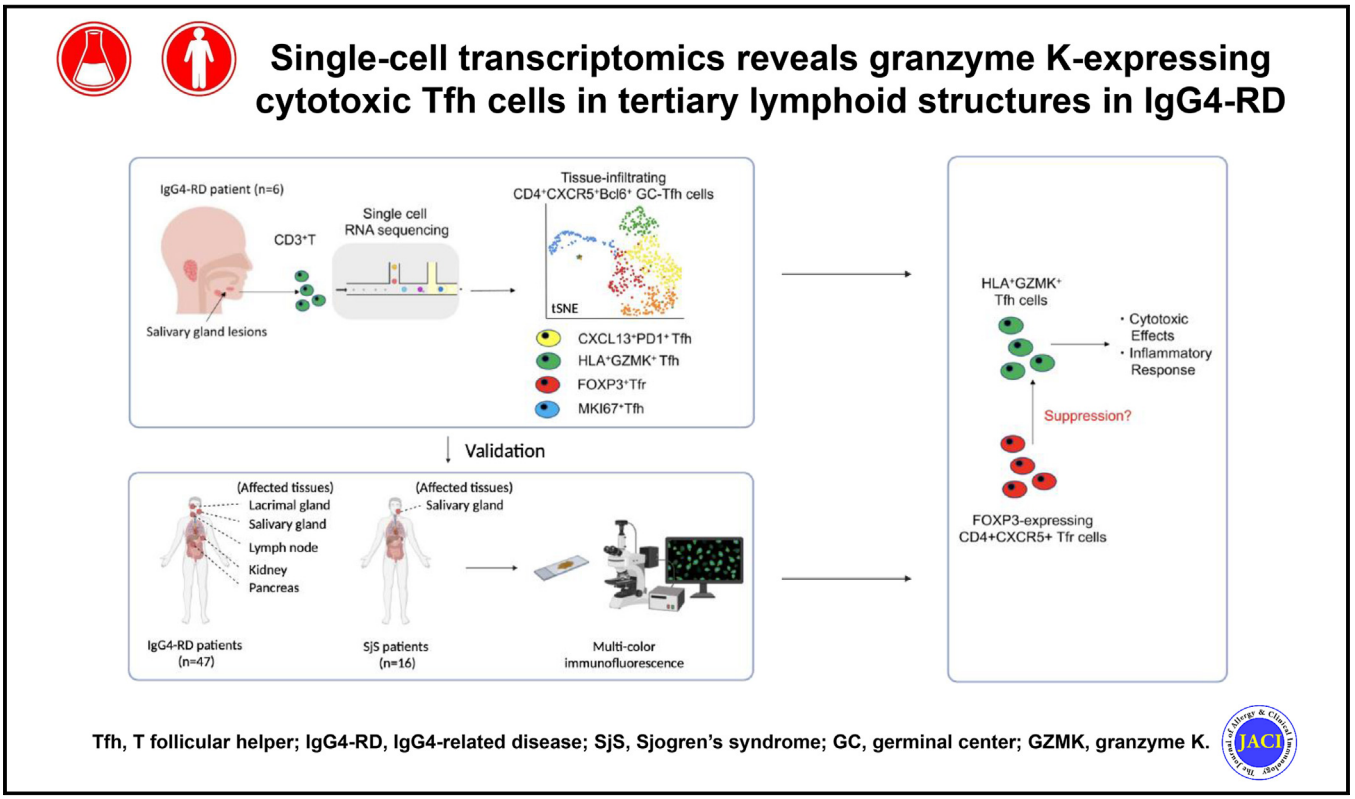

Background: Germinal center (GC) responses controlled by T follicular helper (Tfh) and T follicular regulatory (Tfr) cells are crucial for the generation of high-affinity antibodies. Acquired immune responses to tissue-released antigens might be mainly induced in tertiary lymphoid organs (TLOs) with GCs in affected tissues. IgG4-related disease (IgG4-RD) demonstrates polarized isotype switching and TLOs in affected tissues. We performed single-cell transcriptomics of tissue-infiltrating T cells from these TLOs to obtain a comprehensive, unbiased view of tissue-infiltrating GC-Tfh cells.

From [a]the Section of Oral and Maxillofacial Oncology, Division of Maxillofacial Diagnostic and Surgical Sciences, and [b]the Dento-craniofacial Development and Regeneration Research Center, Faculty of Dental Science, Kyushu University, and [c]Cell Innovator, Inc, Fukuoka, [d]the Graduate School of Medicine, Dentistry & Pharmaceutical Science, Okayama University, Okayama, and [e]the Laboratory of Oral Pathology, Division of Maxillofacial Diagnostic and Surgical Sciences, Faculty of Dental Science, Kyushu University, Fukuoka.

*These authors contributed equally to this work.

Received for publication March 22, 2023; revised August 2, 2023; accepted for publication August 10, 2023.

Corresponding author: Takashi Maehara, DDS, PhD, Section of Oral and Maxillofacial Oncology, Division of Maxillofacial Diagnostic and Surgical Sciences, Faculty of Dental Science, Kyushu University, 3-1-1 Maidashi, Higashi-ku, Fukuoka 812-8582, Japan. E-mail: tmaehara@dent.kyushu-u.ac.jp.

0091-6749/$36.00

https://doi.org/10.1016/j.jaci.2023.08.019

Objective: To identify GC-Tfh-cell subsets in TLOs in patients with IgG4-RD using single-cell transcriptomics.
Methods: Single-cell RNA sequencing of sorted CD3$^+$ T cells and multicolor immunofluorescence analysis were used to investigate CD4$^+$CXCR5$^+$Bcl6$^+$ GC-Tfh cells in affected lesions from patients with IgG4-RD.
Results: Infiltrating CD4$^+$CXCR5$^+$Bcl6$^+$ Tfh cells were divided into 5 main clusters. We detected HLA$^+$ granzyme K$^+$ (GZMK$^+$) Tfh cells with cytotoxicity-associated features in patients with IgG4-RD. We also observed abundant infiltrating Tfr cells with suppressor-associated features in patients with IgG4-RD. These GZMK$^+$ Tfh cells and Tfr cells clustered together in affected tissues from patients with IgG4-RD.
Conclusions: This single-cell data set revealed a novel subset of HLA$^+$GZMK$^+$ cytotoxic Tfh cells infiltrating affected organs in patients with IgG4-RD, suggesting that infiltrating Tfr cells might suppress cytotoxic Tfh cells. (J Allergy Clin Immunol 2023;■■■:■■■-■■■.)

Key words: *Single-cell RNA sequencing, IgG4-related disease, germinal center, granzyme K, T follicular helper cells, T follicular regulatory cells*

Abbreviations used
COVID-19: Coronavirus disease 2019
CTL: Cytotoxic T lymphocyte
GC: Germinal center
GZMB/GZMK: Granzyme B/K
IgG4-RD: IgG4-related disease
scRNA-seq: Single-cell RNA sequencing
SG: Salivary gland
SjS: Sjögren syndrome
SMG: Submandibular gland
Tfh: T follicular helper
Tfr: T follicular regulatory
TLO: Tertiary lymphoid organ

INTRODUCTION

Acquired immune responses are mostly initiated in secondary lymphoid tissues such as lymph nodes. Tertiary lymphoid organs (TLOs) are organized aggregates of immune cells that form in nonlymphoid tissues, and immune responses to some tissue-released antigens are also induced in TLOs with germinal centers (GCs) in affected tissues.[1,2] TLOs arise only in the context of chronic inflammation, such as autoimmune diseases, chronic infections, and cancer.[1,2] T follicular helper (Tfh) cells in GCs within TLOs differ from other CD4$^+$ T cells on the basis of their expression of CXCR5 and Bcl6. They also assist B cells during T-cell–dependent immune responses and contribute to isotype switching, somatic hypermutation, GC formation, and high-affinity B-cell selection in GCs.[3] GC-Tfh cells in TLOs thus play an important role in the immune responses of chronic inflammation; however, the GC-Tfh transcriptome in human diseases is not well understood.

IgG4-related disease (IgG4-RD) is a progressive condition associated with chronic antigen-driven autoimmune activation, resulting in severe fibrosis.[4] We previously identified clonally expanded CD4$^+$ cytotoxic T lymphocytes (CTLs) in blood and affected tissues in patients with IgG4-RD.[5,6] IgG4-RD, systemic sclerosis, fibrosing mediastinitis, and Grave orbitopathy are type 1 immunity-driven fibrotic inflammatory diseases.[6-10] IgG4-RD is characterized by multiorgan inflammation, elevated serum IgG4, IgG4$^+$ plasma cell tissue infiltration, TLOs with GCs, and storiform fibrosis in various organs, including the salivary glands (SGs).[4] Active disease is characterized by circulating expansion of IgG4-expressing plasmablasts,[11] with extensive somatic hypermutation, implying that these B-lineage cells are derived from GCs with the help of GC-Tfh cells. IgG4-RD provides a good disease model to observe the characteristics of GC-Tfh cells because of the swollen affected tissues and formation of numerous TLOs with GCs.

High-dimensional analyses of tissue samples can provide detailed information on infiltrating immune-cell populations in patients with different rheumatic diseases.[12-14] Single-cell RNA sequencing (scRNA-seq) identified distinct clusters of T-cell effector subsets, including T_H1, T_H2, and T_H17 cells. These analyses revealed new effector subsets, including peripheral T_H cells[13] and granzyme K$^+$ (GZMK$^+$) cytotoxic T cells,[12,14] in inflamed tissues from several diseases. Further characterization of accumulated T-cell populations within target tissues will enable precise targeting of biologic therapies and accelerate the development of specific biomarkers to track relevant immune pathways in patients with rheumatic diseases.

Using a single-cell approach, we recently detected a novel subset of IL-10–expressing LAG3$^+$ Tfh-like cells but not regulatory T (Treg) cells or T follicular regulatory (Tfr) cells but expressed CTLA-4 and granzymes in IgG4-RD.[15] Most IL-10$^+$ Tfh-like cells expressed Blimp1 instead of Bcl6 and existed outside GCs in secondary lymphoid organs and TLOs. Extrafollicular B-cell activation was also prominent in IgG4-RD, because isotype switching to IgG4 was driven by IL-10$^+$LAG3$^+$ Tfh-like cells (pre–GC-Tfh cells) outside GCs.[15]

Here, we carried out scRNA-seq to identify GC-Tfh-cell subsets in TLOs in patients with IgG4-RD.

RESULTS AND DISCUSSION

We clarified the role of infiltrating GC-Tfh cells in lesions with TLOs by analyzing CD3$^+$ T cells in SGs from patients with IgG4-RD (n = 6) using scRNA-seq (10x Genomics, Pleasanton, Calif) to profile tissue-infiltrating *CD4*$^+$*CXCR5*$^+$*Bcl6*$^+$ GC-Tfh cells. Patient background and clinical and serological findings are provided in Table E1 (in the Online Repository available at www.jacionline.org). *CD4*$^+$*CXCR5*$^+$*Bcl6*$^+$ GC-Tfh cells clustered into 5 distinct subtypes, visualized by heatmaps and t-distributed stochastic neighbor embedding (Fig 1, *A*). Cluster 0 was characterized by high expression of *PDCD1*, *TOX2*, *ICOS*, *TIGIT*, *CD40LG*, and *CXCL13*, indicating *CXCL13*$^+$*PDCD1*$^+$ Tfh cells (Fig 1, *B* and *C*). Cluster 1 included activated T cells categorized as "unknown" because their gene expression pattern could not be assigned. Cluster 2 was characterized by high expression of *HLA-DRA*, *HLA-DRB1*, *HLA-DQA1*, *HLA-DMA*, *GZMK*, *GZMA*, *TGFB1*, *AREG*, *CST7*, *CRTAM*, *SLAMF7*, *CCL4*, and *CCL5*, indicating activated HLA$^+$ Tfh cells with cytotoxic-related genes.

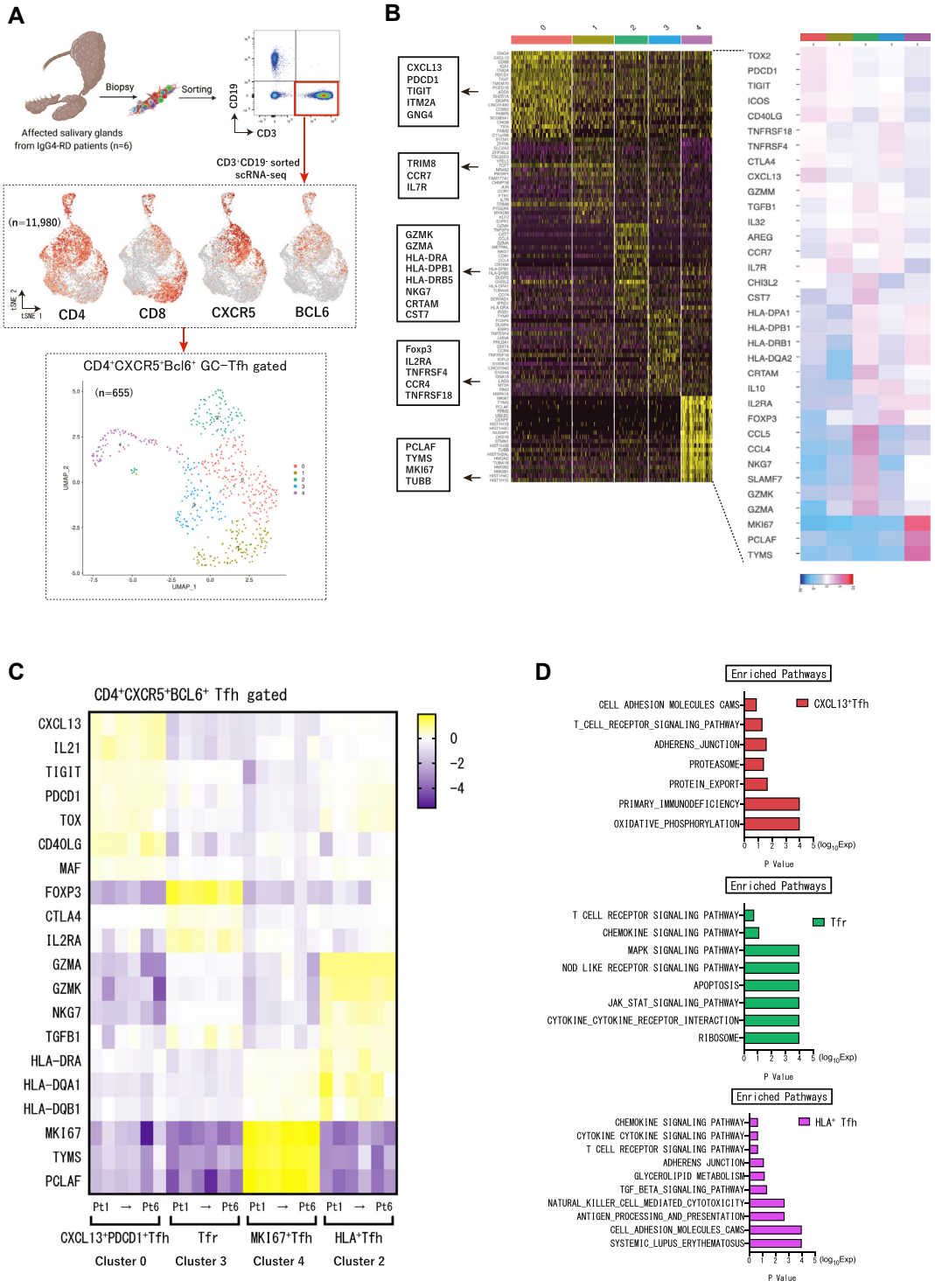

FIG 1. scRNA-seq of tissue-infiltrating *CD4*$^+$ *CXCR5*$^+$ *Bcl6*$^+$ T cells in IgG4-RD tissues with TLOs. **A,** Schematic of experimental protocol. CD3$^+$ T cells and CD19$^+$ B cells were sorted in SMGs from 6 patients with IgG4-RD. tSNE of single-cell expression profiles (n = 11,980); *CD4*$^+$ *CXCR5*$^+$ *Bcl6*$^+$-gated GC-Tfh cells were separated into 5 clusters. Schematic representation of clustering of *CD4*$^+$ *CXCR5*$^+$ *Bcl6*$^+$ GC-Tfh cells in a patient with IgG4-RD (Pt 5). **B,** Heatmaps showing (*left*) expression patterns of top 20 genes and (*right*) marker genes in *CD4*$^+$ *CXCR5*$^+$ *Bcl6*$^+$ GC-Tfh cells among 5 clusters in a patient with IgG4-RD (Pt 5). **C,** Heatmap showing marker genes in *CD4*$^+$ *CXCR5*$^+$ *Bcl6*$^+$ GC-Tfh cells among 4 clusters (*CXCL13*$^+$ *PDCD1*$^+$ Tfh, Tfr, *MKI67*$^+$ Tfh, *HLA*$^+$ *GZMK*$^+$ cytotoxic Tfh) in 6 patients with IgG4-RD. **D,** Gene set enrichment analysis and unique inflammatory response pathways for genes in 3 clusters (*CXCL13*$^+$ *PDCD1*$^+$ Tfh, Tfr, *HLA*$^+$ *GZMK*$^+$ cytotoxic Tfh) in IgG4-RD. Significantly enriched gene sets for each cell subset shown (terms selected from significantly enriched gene sets for each cell subset and gene set [false-discovery rate < 0.05]). Bar charts show significant upregulation in a cluster compared with other clusters. *JAK-STAT,* Janus kinase–signal transducer and activator of transcription, *MAPK,* mitogen-activated protein kinase; *NOD,* nucleotide oligomerization domain; *tSNE*, t-Distributed stochastic neighbor embedding.

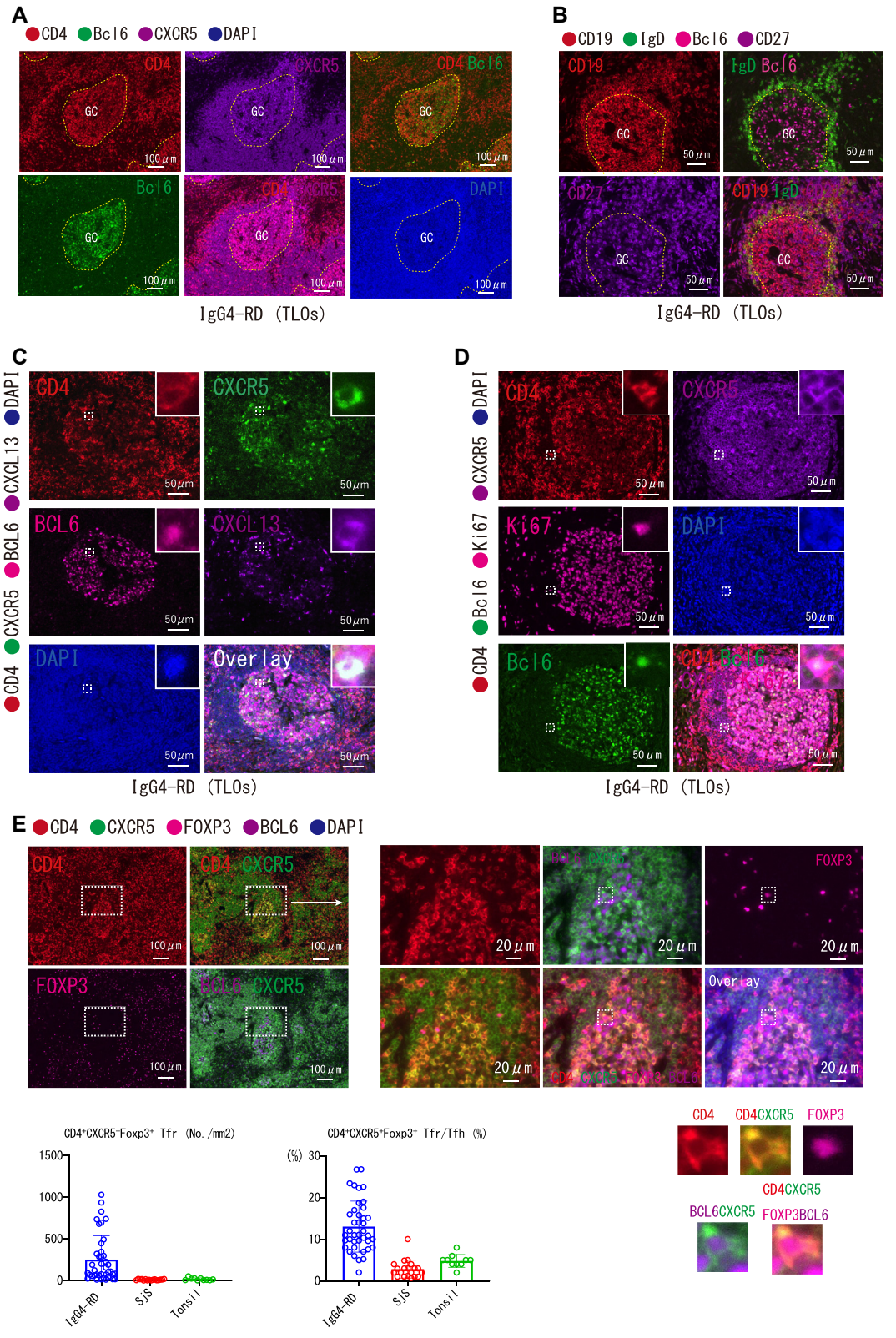

FIG 2. Multicolor immunofluorescence examination of GC-Tfh-cell subsets in TLOs from IgG4-RD tissues. Immunofluorescence staining of (**A**) CD4 (*red*), Bcl6 (*green*), CXCR5 (*magenta*), and DAPI (*blue*) and (**B**) CD19 (*red*), IgD (*green*), Bcl6 (*pink*), and CD27 (*magenta*) in SG from a patient with IgG4-RD. *Yellow broken lines* show GCs. **C,** Immunofluorescence staining of CD4 (*red*), CXCR5 (*green*), Bcl6 (*pink*), CXCL13 (*magenta*), and DAPI (*blue*) in SG from a patient with IgG4-RD. *White boxes*: $CD4^+CXCR5^+Bcl6^+CXCL13^+$ Tfh. **D,** Immunofluorescence staining of CD4 (*red*), Bcl6 (*green*), Ki67 (*pink*), CXCR5 (*magenta*), and DAPI

Cluster 3 was characterized by high expression of *FOXP3*, *CTLA4*, *IL2RA*, *TNFRSF4*, *TNFRSF18*, and *IL10*, indicating Tfr cells. Cluster 4 was characterized by high expression of *MKI67*, *PCLAF*, and *TYMS*, indicating a proliferating subset of GC-Tfh cells. All clusters contained cells from each of the 6 patients.

We examined the molecular signaling pathways in these cells (Fig 1, *D*). Oxidative phosphorylation, primary immunodeficiency, protein export, proteasome, adherens junctions, and T-cell receptor signaling and cell adhesion molecules pathways were all significantly upregulated in *CXCL13*$^+$*PDCD1*$^+$*TIGIT*$^+$ GC-Tfh cells. Cell adhesion molecules, antigen processing and presentation, natural killer cell–mediated cytotoxicity, TGF-β signaling, adherens junctions, and T-cell receptor, cytokine-cytokine, and chemokine signaling pathways were all significantly upregulated in HLA$^+$ cytotoxic GC-Tfh cells. Ribosome, cytokine-cytokine receptor interaction, apoptosis, and Janus kinase–signal transducer and activator of transcription, nucleotide oligomerization domain (NOD)-like receptor, mitogen-activated protein kinase, chemokine, and T-cell receptor signaling pathways were all significantly upregulated in GC-Tfr cells.

Combined analysis of several markers revealed GC-Tfh cells in TLOs with GCs. We then analyzed affected TLOs with GCs from patients with IgG4-RD. GC-Tfh cells and ectopic GCs were identified by multicolor immunofluorescence (CD4, CXCR5, Bcl6, and 4'-6-diamidino-2-phenylindole [Fig 2, *A*] and CD19, IgD, Bcl6, CD27, and 4'-6-diamidino-2-phenylindole [Fig 2, *B*], respectively). Multicolor staining revealed that CD4 Bcl6$^+$CXCR5$^+$ GC-Tfh cells in IgG4-RD TLOs with GCs expressed CXCL13 or Ki67 (Fig 2, *C* and *D*), and some CD4$^+$Bcl6$^+$CXCR5$^+$ GC-Tfh cells also expressed FOXP3 (Fig 2, *E*). FOXP3-expressing CD4$^+$CXCR5$^+$ Tfr cells were abundant in IgG4-RD lesions but were sparse in Sjögren syndrome (SjS) and healthy tonsils (Fig 2, *E*). Patient background and clinical and serological findings are provided in Tables E2 and E3 (in the Online Repository available at www.jacionline.org). Kimura's disease (KD) is a chronic inflammatory fibrotic disorder that involves subcutaneous eosinophilic lymph follicular granulomas and high serum IgE levels and we recently reported that allergic fibrosis from KD may be driven by type 2 immune cells.[15] By using multicolor staining, GATA3$^+$ GC-Tfh cells were abundant in TLOs from patients with KD, but not in IgG4-RD (see Fig E1 in this article's Online Repository at www.jacionline.org).

We used an *in silico* approach (CellPhoneDB v3.0; Sanger Institute, Cambridgeshire, United Kingdom) to predict potential cell-cell interaction pairs on the basis of unbiased ligand-receptor interaction analyses between Tfr cells and other effector Tfh cells.[16] Tfr cells did not interact with the undefined cluster (cluster 1) (see Fig E2 in this article's Online Repository at www.jacionline.org). Notably, this approach was based on databases of biochemically deduced protein-protein interactions, and some of the predictions may not be biologically meaningful. However, the *CTLA4-CD80*, *TNFSF9-TNFRSF9*, and *IL10 receptor–IL10* interactions between Tfr cells and HLA$^+$ cytotoxic Tfh cells are likely to be accurate (Fig 3, *A*). Multicolor staining revealed that GZMK$^+$ cytotoxic Tfh cells and Tfr cells clustered together in IgG4-RD tissues (Fig 3, *B* and see Fig E3 in this article's Online Repository at www.jacionline.org).

The regulatory mechanism of Tfr cells depends on coinhibitory receptors, inhibitory cytokines, and granzyme release. CTLA-4 is a direct suppressor of Tfh cells, limits the expression of costimulatory ligands CD80 and CD86 on B cells, and controls the overreaction of GCs. We examined marker gene (*CTLA4*, *IL2RA*, *TGFB1*, *ICOS*, *TNFRSF4*, *TNFRSF9*, *TNFRSF18*, and *CCR7*) expression in gated IgG4-RD *CD4*$^+$*CXCR5*$^+$*FOXP3*$^+$ Tfr cells (Fig 3, *C*). Tfr cells repress the development of abnormal granzyme B (GZMB)-expressing cytotoxic Tfh cells and promote GC responses and the production of high-affinity autoantibodies.[17] Tfr-cell expansion may reflect regulatory/feedback processes designed to promote immune tolerance and control excessive and inappropriate inflammation mediated by effector GZMK$^+$ Tfh cells.

Cytotoxic Tfh cells and CD4$^+$ CTLs in blood from patients with severe coronavirus disease 2019 (COVID-19) were also expanded.[18] In this report, the expanded cytotoxic Tfh cells expressed several transcripts encoding for molecules linked to inhibitory function, such as TIGIT, LAG3, TIM3, and PD1, and to negative regulation of T-cell activation and proliferation, such as DUSP4 and CD70, suggesting that these cytotoxic Tfh cells were "dysfunctional" or "exhausted" as stated in previous reports.[2,3] In this report, the transcriptomic features of COVID-19–reactive CD4$^+$ CTLs and cytotoxic Tfh cells suggest that they are likely to play an important role in orchestrating immune responses by recruiting innate immune cells to enhance CD8$^+$ T-cell responses while also directly mediating cytotoxic death of MHC class II–expressing virally infected cells.

In our scRNA-seq, HLA$^+$GZMK$^+$ cytotoxic Tfh cells in IgG4-RD do not express immune checkpoint-related genes (PDCD1, TIGIT, LAG3, and TIM3) but express cytotoxic molecules (GZMA, GZMM, IFN-γ, CRTAM, SLAMF7, CCL4, CCL5, NKG7, and CST7), suggesting that these are effector T-cell subsets. Furthermore, these HLA$^+$GZMK$^+$ cytotoxic Tfh cells express some fibrotic-related genes (amphiregulin and TGF-β). Because previous reports have shown that circulating CD4$^+$ CTLs were increased in blood from patients with IgG4-RD, a comparative study of gene expression between infiltrating CD4$^+$ CTLs and HLA$^+$GZMK$^+$ cytotoxic Tfh cells at the single-cell level is needed. These HLA$^+$GZMK$^+$ cytotoxic Tfh cells with CD4$^+$ CTLs in lesions will be more thoroughly investigated in future studies.

We recently detected a novel subset of IL-10–expressing LAG3$^+$ICOS$^+$ Tfh-like cells in IgG4-RD, expressing IL-21 and CTLA-4 but not FOXP3, suggesting that they were not phenotypic Treg or Tfr cells.[15] Here, we compared IL-10–expressing T cells among IL-10$^+$ Tfh-like, IL-10$^+$ Treg, and IL-10$^+$ Tfr cells using quantitative tissue immunofluorescence. IL-10$^+$LAG3$^+$CD4$^+$CXCR5$^+$ Tfh-like cells were more abundant

(*blue*) in affected SG from a patient with IgG4-RD. *White boxes*: CD4$^+$CXCR5$^+$Bcl6$^+$Ki67$^+$ Tfh. **E,** *Upper*: Immunofluorescence staining of CD4 (*red*), CXCR5 (*green*), FOXP3 (*pink*), Bcl6 (*magenta*), and DAPI (*blue*) in affected SG from a patient with IgG4-RD. *White boxes*: CD4$^+$CXCR5$^+$Bcl6$^+$FOXP3$^+$ Tfr. *Lower*: Quantitative analysis of CD4$^+$CXCR5$^+$FOXP3$^+$ Tfr and CD4$^+$CXCR5$^+$FOXP3$^-$ Tfh-cell subsets in lacrimal glands, draining lymph nodes, kidney tissues, and SGs from 47 patients with IgG4-RD, 16 patients with SjS, and 10 healthy subjects by multicolor immunofluorescence. *DAPI*, 4'-6-Diamidino-2-phenylindole.

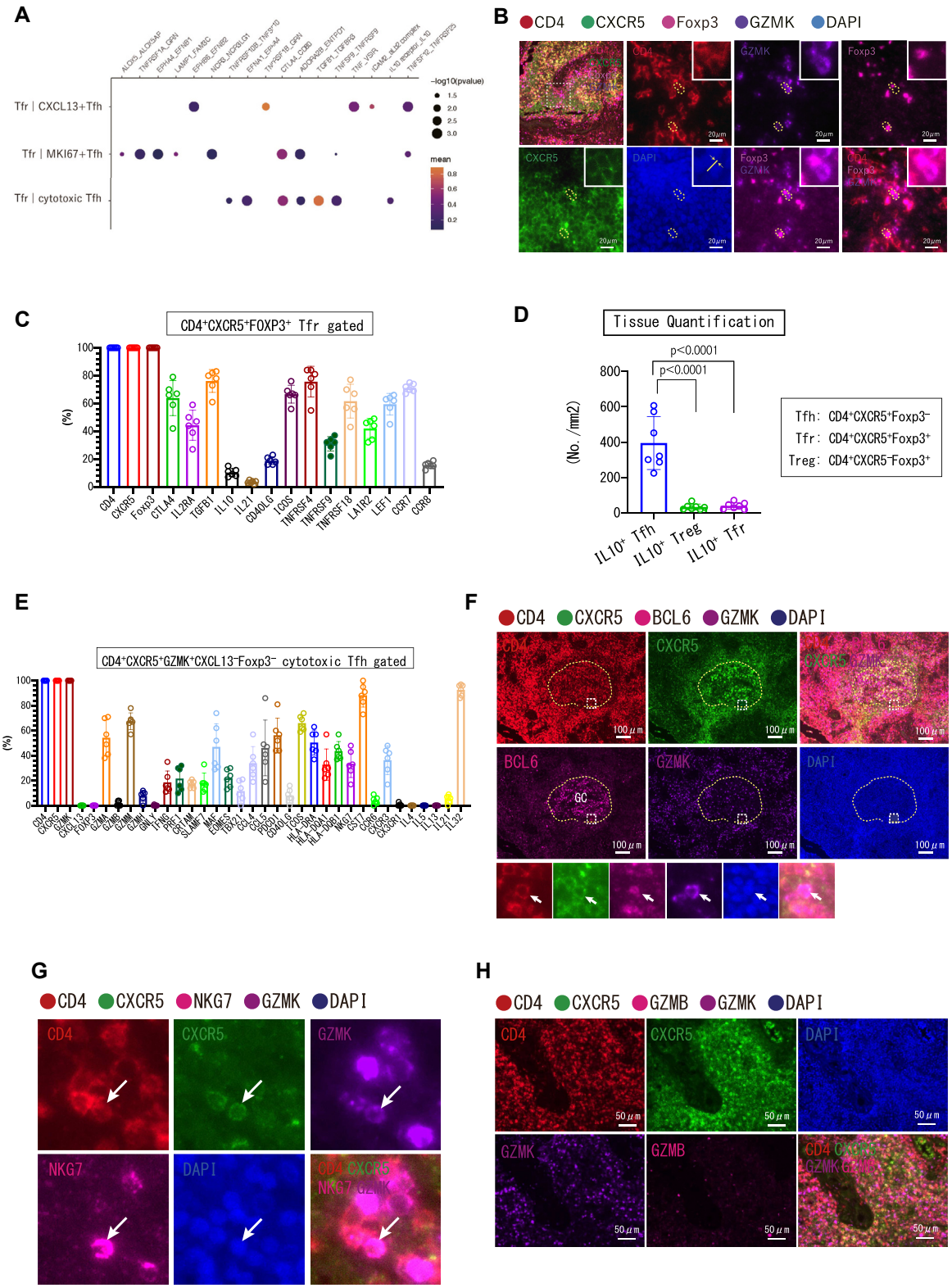

FIG 3. Lesional GZMK$^+$ cytotoxic Tfh cells and IL-10$^+$LAG3$^+$ Tfh-like cells in IgG4-RD tissues. **A,** Dot plot of ligand-receptor interactions between Tfr cells and activated Tfh cells in different clusters (cluster 0: CXCL13$^+$ Tfh; cluster 2: HLA$^+$ cytotoxic Tfh; and cluster 4: MKI67$^+$ Tfh). **B,** Immunofluorescence staining of CD4 (*red*), FOXP3 (*pink*), GZMK (*magenta*), CXCR5 (*green*), and DAPI (*blue*) and visualization of T-B conjugates in SMG from a patient with IgG4-RD using StrataQuest cell-to-cell contact application (Tissue Gnostics, Brisbane, Australia). Nuclei circled in *yellow* depict CD4$^+$GZMK$^+$ CTLs and CD4$^+$FOXP3$^+$ Treg cells, respectively, in T-B conjugates. CD4$^+$GZMK$^+$ CTLs and CD4$^+$FOXP3$^+$ Treg cells clustered together. **C,** Expression of marker genes in *CD4*$^+$ *CXCR5*$^+$ *FOXP3*$^+$ Tfr cells in SGs from 6 patients with IgG4-RD by scRNA-seq. **D,** Quantitative

than IL-10$^+$CD4$^+$CXCR5$^-$FOXP3$^+$ Treg cells or IL-10$^+$CD4$^+$CXCR5$^+$FOXP3$^+$ Tfr cells (Fig 3, *D*).

The reason for the increase in IL-10$^+$LAG3$^+$ Tfh-like cells with suppressor-associated features is unclear, but some antigens may be overexpressed in apoptotic cells via antigen-specific clonally expanded CD4/CD8$^+$ CTLs in IgG4-RD.[5,10] Endothelial cells are a common target of apoptosis in systemic sclerosis,[7] consistent with clinical vasculopathy, whereas nonendothelial, nonimmune, vimentin-positive mesenchymal cells were the most frequent apoptotic cell type in IgG4-RD, with a higher frequency compared with chronic sialadenitis or SjS.[7,10] Given the pathogenesis of IgG4-RD, we presume that prolonged activation of CD4$^+$ T cells by persistent antigens facilitates the differentiation of appropriate IL-10$^+$LAG3$^+$ Tfh-like cells that drive IgG4 class switching, and these cells may collaborate with reactivated B cells that have already switched to other IgG subtypes.[19] Indolent, gradual, inflammatory processes, driven largely by infiltrating T and B cells, can generate a suitable milieu for the expansion of extrafollicular T_H cells that drive IgG4 switching in IgG4-RD.[20] However, further studies of IL-10$^+$LAG3$^+$ Tfh-like cells are required to clarify the pathogenesis of IgG4-RD.

We previously showed that cytotoxic-phenotype IgG4-RD Tfh cells share some genes (*SLAMF7*, *CRTAM*, *NKG7*, *GZMA*, *GZMK*, *CCL4*, and *CCL5*).[15] We then examined the GZMK$^+$ cytotoxic Tfh-cell transcriptome, given that cytotoxic Tfh cells are also known to be expanded in diseases such as severe COVID-19.[18] Here, we visualized selected marker genes in gated infiltrating *CD4*$^+$*CXCR5*$^+$*GZMK*$^+$*CXCL13*$^-$*FOXP3*$^-$ cytotoxic Tfh cells from IgG4-RD tissues. These cells expressed *GZMA*, *GZMM*, *IFN-γ*, *PRF1*, *CRTAM*, *SLAMF7*, *MAF*, *CCL4*, *CCL5*, *PDCD1*, *ICOS*, *HLA*, *NKG7*, and *CST7*, but not *GZMB*, *GZMH*, *GNLY*, *CD40LG*, *CX3CR1*, *IL4*, *IL5*, *IL13*, or *IL21* (Fig 3, *E*). Multicolor staining revealed CD4$^+$CXCR5$^+$BCL6$^+$GZMK$^+$ and CD4$^+$CXCR5$^+$NKG7$^+$GZMK$^+$ Tfh cells in IgG4-RD tissues (Fig 3, *F* and *G*). GZMK$^+$CD4$^+$CXCR5$^+$ Tfh cells were in physical contact with cleaved caspase 3–expressing cells (see Fig E4 in this article's Online Repository at www.jacionline.org). CD4$^+$CXCR5$^+$GZMK$^+$ cytotoxic Tfh cells did not express GZMB (Fig 3, *H*). By using multi-color staining, CD4$^+$CXCR5$^+$HLA-DR$^+$GZMK$^+$ Tfh cells were clearly detected in IgG4-RD tissues and these Tfh cells were quantified (see Fig E5 in this article's Online Repository at www.jacionline.org).

A distinct GZMK$^+$CD4$^+$ and CD8$^+$ T-cell cluster was also observed in lupus nephritis and rheumatoid arthritis, with almost no overlap with GZMB expression.[21,22] Understanding the roles of GZMK$^+$ cells in inflamed tissues is of major interest, and additional research on GZMK$^+$ T cells, including CD4$^+$ CTLs, CD8$^+$ CTLs, and GZMK$^+$ Tfh cells, is required to clarify the pathogenesis of inflammatory disorders.

We demonstrated the presence of GC-Tfh subsets in IgG4-RD TLOs with GCs, using scRNA-seq and multiple immunofluorescence. We also showed that tissue-infiltrating GC-Tfh cells were heterogeneous, and GZMK$^+$HLA$^+$ cytotoxic Tfh cells were similar to a subset described in other diseases, including severe COVID-19.[18] We also identified a prominent subset of infiltrating Tfr cells with suppressor-associated and cytotoxic-associated features in IgG4-RD.

DISCLOSURE STATEMENT

This study was supported by grants from Japan Society for the Promotion of Science KAKENHI (grant nos. JP21K19607, JP18KK0260, and JP19H03854 to T.M. and grant no. JP20H00553 to S.N.) and Takeda Foundation (FBKF511822 to T.M.).

Disclosure of potential conflict of interest: The authors declare that they have no relevant conflicts of interest.

We thank Susan Furness, PhD, from Edanz (https://jp.edanz.com/ac) for editing a draft of this article. All tissue-quantification data were shared in TissueGnostics Software at Kyushu University and the Ragon Institute of MGH, MIT, and Harvard.

Key messages

- **scRNA-seq provides an unbiased and unprecedented view of infiltrating GC-Tfh-cell subsets in TLOs from IgG4-RD lesions.**
- **Our analysis provides that GZMK$^+$ Tfh cells and Tfr cells clustered together in IgG4-RD TLOs, suggesting that infiltrating Tfr cells might suppress cytotoxic Tfh cells in patients with IgG4-RD.**

REFERENCES

1. Pitzalis C, Jones GW, Bombardieri M, Jones SA. Ectopic lymphoid-like structures in infection, cancer and autoimmunity. Nat Rev Immunol 2014;14:447-62.
2. Schumacher TN, Thommen DS. Tertiary lymphoid structures in cancer. Science 2022;375:eabf9419.
3. Crotty S. A brief history of T cell help to B cells. Nat Rev Immunol 2015;15:185-9.
4. Kamisawa T, Zen Y, Pillai S, Stone JH. IgG4-related disease. Lancet 2015;385:1460-71.
5. Mattoo H, Mahajan VS, Maehara T, Deshpande V, Della-Torre E, Wallace ZS, et al. Clonal expansion of CD4(+) cytotoxic T lymphocytes in patients with IgG4-related disease. J Allergy Clin Immunol 2016;138:825-38.
6. Maehara T, Mattoo H, Ohta M, Mahajan VS, Moriyama M, Yamauchi M, et al. Lesional CD4+ IFN-γ+ cytotoxic T lymphocytes in IgG4-related dacryoadenitis and sialoadenitis. Ann Rheum Dis 2017;76:377-85.
7. Maehara T, Kaneko N, Perugino CA, Mattoo H, Kers J, Allard-Chamard H, et al. Cytotoxic CD4+ T lymphocytes may induce endothelial cell apoptosis in systemic sclerosis. J Clin Invest 2020;130:2451-64.
8. Wang Y, Chen Z, Wang T, Guo H, Liu Y, Dang N, et al. A novel CD4+ CTL subtype characterized by chemotaxis and inflammation is involved in the pathogenesis of Graves' orbitopathy. Cell Mol Immunol 2021;18:735-45.

analysis of IL-10$^+$CD4$^+$CXCR5$^+$LAG3$^+$ Tfh-like, IL-10$^+$CD4$^+$CXCR5$^-$FOXP3$^+$ Treg, and IL-10$^+$CD4$^+$CXCR5$^+$FOXP3$^+$ Tfr-cell subsets in lacrimal glands and SGs from 7 patients with IgG4-RD by multicolor immunofluorescence. **E,** Expression patterns of marker genes in *CD4*$^+$ *CXCR5*$^+$ *GZMK*$^+$ *CXCL13*$^-$*FOXP3*$^-$ Tfh cells in SGs from 6 patients with IgG4-RD by scRNA-seq. Immunofluorescence staining of (**F**) CD4 (*red*), CXCR5 (*green*), BCL6 (*pink*), NKG7 (*magenta*), and DAPI (*blue*) (*white boxes*: CD4$^+$CXCR5$^+$GZMK$^+$BCL6$^+$ Tfh), (**G**) CD4 (*red*), CXCR5 (*green*), CXCR5 (*pink*), NKG7 (*magenta*), and DAPI (*blue*) (white boxes: CD4$^+$CXCR5$^+$GZMK$^+$NKG7$^+$ Tfh), and (**H**) CD4 (*red*), CXCR5 (*green*), GZMB (*pink*), GZMK (*magenta*), and DAPI (*blue*) in SGs from a patient with IgG4-RD. *DAPI*, 4′-6-Diamidino-2-phenylindole.

9. Allard-Chamard H, Alsufyani F, Kaneko N, Xing K, Perugino C, Mahajan VS, et al. CD4(+)CTLs in fibrosing mediastinitis linked to histoplasma capsulatum. J Immunol 2021;206:524-30.
10. Perugino CA, Kaneko N, Maehara T, Mattoo H, Kers J, Allard-Chamard H, et al. CD4(+) and CD8(+) cytotoxic T lymphocytes may induce mesenchymal cell apoptosis in IgG(4)-related disease. J Allergy Clin Immunol 2021;147:368-82.
11. Mattoo H, Mahajan VS, Della-Torre E, Sekigami Y, Carruthers M, Wallace ZS, et al. De novo oligoclonal expansions of circulating plasmablasts in active and relapsing IgG4-related disease. J Allergy Clin Immunol 2014;134:679-87.
12. Arazi A, Rao DA, Berthier CC, Davidson A, Liu Y, Hoover PJ, et al. The immune cell landscape in kidneys of patients with lupus nephritis. Nat Immunol 2019;20:902-14.
13. Rao DA, Gurish MF, Marshall JL, Slowikowski K, Fonseka CY, Liu Y, et al. Pathologically expanded peripheral T helper cell subset drives B cells in rheumatoid arthritis. Nature 2017;542:110-4.
14. Zhang F, Wei K, Slowikowski K, Fonseka CY, Rao DA, Kelly S, et al. Defining inflammatory cell states in rheumatoid arthritis joint synovial tissues by integrating single-cell transcriptomics and mass cytometry. Nat Immunol 2019;20:928-42.
15. Munemura R, Maehara T, Murakami Y, Koga R, Aoyagi R, Kaneko N, et al. Distinct disease-specific Tfh cell populations in two different fibrotic diseases: IgG4-related disease and Kimura's disease. J Allergy Clin Immunol 2022;150:440-55.e17.
16. Efremova M, Vento-Tormo M, Teichmann SA, Vento-Tormo R. CellPhoneDB: inferring cell-cell communication from combined expression of multi-subunit ligand-receptor complexes. Nat Protoc 2020;15:1484-506.
17. Xie MM, Fang S, Chen Q, Liu H, Wan J, Dent AL. Follicular regulatory T cells inhibit the development of granzyme B-expressing follicular helper T cells. JCI Insight 2019;4:e128076.
18. Meckiff BJ, Ramírez-Suástegui C, Fajardo V, Chee SJ, Kusnadi A, Simon H, et al. Imbalance of regulatory and cytotoxic SARS-CoV-2-reactive CD4(+) T cells in COVID-19. Cell 2020;183:1340-53.e16.
19. Horns F, Vollmers C, Croote D, Mackey SF, Swan GE, Dekker CL, et al. Lineage tracing of human B cells reveals the in vivo landscape of human antibody class switching. Elife 2016;5:e16578.
20. Pillai S. Is it bad, is it good, or is IgG4 just misunderstood? Sci Immunol 2023;8:eadg7327.
21. Jonsson AH, Zhang F, Dunlap G, Gomez-Rivas E, Watts GFM, Faust HJ, et al. Granzyme K(+) CD8 T cells form a core population in inflamed human tissue. Sci Transl Med 2022;14:eabo0686.
22. Gao Y, Dunlap G, Elahee M, Rao DA. Patterns of T-cell phenotypes in rheumatic diseases from single-cell studies of tissue. ACR Open Rheumatol 2021;3:601-13.

METHODS

Study population

We included 47 patients with IgG4-RD and 16 with active SjS. All patients were followed up at the Department of Oral and Maxillofacial Surgery of Kyushu University Hospital, a tertiary care center, between 2010 and 2022. Open submandibular gland (SMG) biopsies were obtained from 30 patients with IgG4-RD on the basis of a previously published protocol, and lacrimal glands, draining lymph nodes, and kidney tissues were also obtained from 17 patients with IgG4-RD. In addition, 10 histologically normal healthy human tonsils were obtained. IgG4-RD was diagnosed according to the following criteria: (1) persistent (>3 months) symmetrical swelling of more than 2 lacrimal and major SGs, (2) high (>135 mg/dL) serum IgG4, and (3) tissue infiltration of $IgG4^+$ plasma cells ($IgG4^+$ cells/IgG^+ cells, >40%) determined by immunostaining.[E1] All SMGs from patients with IgG4-RD had histopathologic features of IgG4-RD. SjS was diagnosed as described previously. All patients exhibited objective evidence of SG involvement on the basis of the presence of subjective xerostomia and a decreased salivary flow rate, abnormal findings on parotid sialography, and focal lymphocytic infiltrates in labial SGs. None of the patients with IgG4-RD or SjS had a history of treatment with steroids or other immunosuppressants, infection with HIV, hepatitis B virus, or hepatitis C virus, or sarcoidosis or evidence of lymphoma at the time of the study. All patients with IgG4-RD or SjS had extensive tissue lymphocytic infiltration. It was not appropriate or possible to involve the patients in the design, processing, reporting, or dissemination plans for this study.

Affected SGs, lacrimal glands, lymph nodes, and pancreas samples were obtained from Kyushu University Hospital. Normal human tonsil samples were obtained from Massachusetts General Hospital. Kidney tissues from patients with IgG4-RD were provided from Kanazawa University Hospital. Background and clinical and serological findings for all patients with IgG4-RD and SjS in this study are provided in Tables E1 to E3.

This study protocol was approved by the Institutional Review Board of the Center for Clinical and Translational Research of Kyushu University Hospital (approval no. 834-00) and followed the tenets of the Declaration of Helsinki. All participants provided informed written consent.

Single-cell RNA sequencing

IgG4-RD tissue samples (n = 6) for scRNA-seq were roughly divided, degraded with enzymes, and manually disrupted into a suspension by processing through a 100-μm strainer with a syringe plunger. $CD19^-CD3^+$ T cells and $CD3^-CD19^+$ B cells were prepared from SMGs from a patient with IgG4-RD by positive selection using EasySep Human CD3 and CD19 Positive Selection Kit II (STEMCELL Technologies, Vancouver, British Columbia, Canada) in accordance with the manufacturer's instructions.

scRNA-seq transcriptomics of infiltrating lymphocytes from affected SGs in patients with IgG4-RD

Single-cell library preparation was performed using Chromium Next GEM Single-Cell 5′ Library & Gel Bead Kit v1.1 (10x Genomics, Pleasanton, Calif). Cell suspensions were loaded onto a chromium single-cell chip along with the reverse transcription master mix and single-cell 5′ gel beads at a target concentration of 5000 cells per channel. Following the generation of single-cell gel bead-in-emulsions, reverse transcription was performed using a Bio-Rad T-100 thermal cycler (Bio-Rad Laboratories, Hercules, Calif). Sixteen cycles were performed for cDNA amplification. To construct the gene expression library, cDNA was processed using Chromium Single-Cell 5′ Library Construction Kit (10x Genomics) in accordance with the manufacturer's instructions, including 14 amplification cycles. Libraries were converted using MGIEasy Universal Library Conversion Kit (MGI Tech Co, Ltd, Shenzhen, China) and sequenced on an MGI DNBSEQ-G400 sequencer (MGI Tech Co, Ltd) using a 150 paired-end sequencing kit.

Immunohistochemical analysis

Formalin-fixed and paraffin-embedded sections (4-μm thick) were prepared and stained using a conventional avidin-biotin complex technique. Sections were incubated with IgG4 rabbit mAbs (clone: EP4420; Abcam, Waltham, Mass). Tissue sections were incubated with primary antibodies for 2 hours followed by biotinylated anti–mouse and rabbit secondary antibodies (Vector, Newark, Calif), and then counterstained with Mayer hematoxylin.

Multicolor immunofluorescence staining

Formalin-fixed, paraffin-embedded tissue samples were sectioned at 4 μm and incubated with primary antibodies specific for the following proteins: CD4 (clone: EPR6855; Abcam), GZMK (clone: EPR24601-164, catalog no.: ab282703; Abcam), CXCR5 (clone: MAB190; R&D Systems), CD19 (clone: EPR5906, catalog no.: ab134114; Abcam), CD27 (clone: EPR8569, catalog no.: ab131254; Abcam), Ki67 (clone: SP6, catalog no.: ab16667; Abcam), IgD (catalog no.: BSB 5666; Bio SB), BCL6 (clone: LN22; Biocare Medical, Pacheco, Calif), NKG7 (clone: E6S2A, catalog no.: 84835; Cell Signaling Technology, Danvers, Mass), CXCL13 (clone: EPR23400-92, catalog no.: ab246518; Abcam), IL-10 (catalog no.: ab34843; Abcam), LAG3 (catalog no.: ab209236; Abcam), HLA-DRA (catalog no.: ab92511; Abcam), cleaved caspase 3 (catalog no.: ab32351; Abcam), and FOXP3 (catalog no.: 98377; Cell Signaling Technology). Specimens were then incubated with secondary antibody using an Opal Multiplex Kit (Perkin Elmer, Waltham, Mass). The samples were mounted with the ProLong Diamond Antifade mountant containing 4′-6-diamidino-2-phenylindole (Invitrogen, Waltham, Mass).

Microscopy and quantitative analysis

Images of tissue specimens were acquired using the TissueFAXS platform (Tissue Gnostics, Brisbane, Australia). For quantitative analysis, the entire tissue area was acquired as digital grayscale images in 5 channels with filter settings for fluorescein isothiocyanate, Cy3, Cy5, Cy7, and 4′-6-diamidino-2-phenylindole. Specific cell phenotypes were identified and quantified using the TissueQuest software (TissueGnostics), with cutoff values determined relative to positive controls. This microscopy-based multicolor tissue cytometry software permits multicolor analysis of single cells within tissue sections, in a manner similar to that for flow cytometry. The principle of the method and the algorithms used have been described in detail elsewhere.

Sequencing data analysis

Sample demultiplexing, alignment to the mm 10 reference genome, barcode/unique molecular identifier processing, and gene counting for each cell were performed using the 10x Genomics Cell Ranger pipeline (v5.0.0). The Seurat package (v4.0; Satija Lab, New York, NY) was used for quality checking, filtering, normalization, clustering analyses, and visualization.

Statistical analysis

GraphPad Prism 8 (GraphPad Software; Boston, Mass) was used for statistical analysis, curve fitting, and linear regression. *P* values for continuous, nonparametric variables were calculated using the Mann-Whitney *U* test, Spearman rank correlations, ANOVA, and the Student *t* test. All statistical analyses were performed using JMP Pro software v16 (SAS Institute, Cary, NC). The Kruskal-Wallis test was used to compare more than 1 population. A *P* value of less than .05 was considered statistically significant.

REFERENCE

E1. Umehara H, Okazaki K, Masaki Y, Kawano M, Yamamoto M, Saeki T, et al. A novel clinical entity, IgG4-related disease (IgG4RD): general concept and details. Mod Rheumatol 2012;22:1-14.

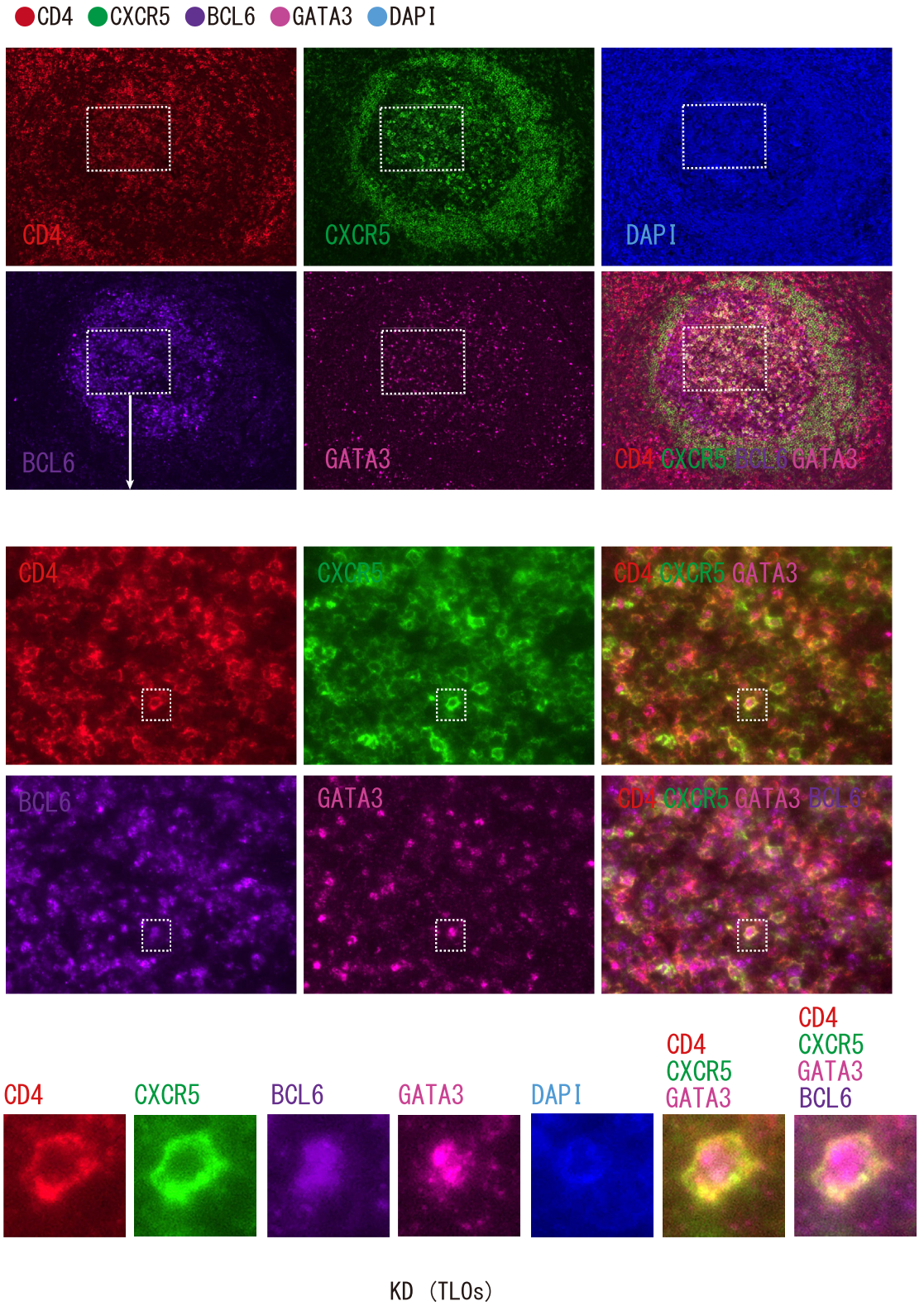

FIG E1. $CD4^+CXCR5^+GATA3^+BCL6^+$ GC-Tfh cells were abundant in TLOs from patients with Kimura disease. Immunofluorescence staining of CD4 (*red*), CXCR5 (*green*), Bcl6 (*purple*), GATA3 (*pink*), and DAPI (*blue*) in affected tissues from a patient with Kimura disease. *DAPI*, 4′-6-Diamidino-2-phenylindole.

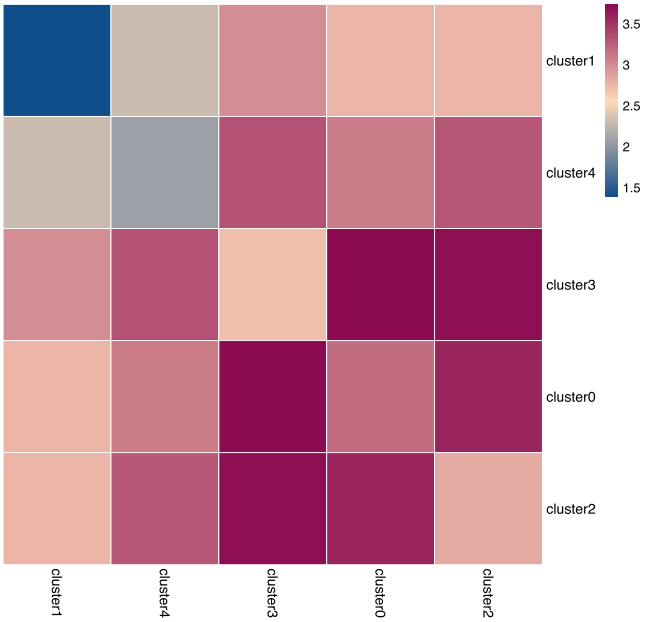

FIG E2. Imputation of interactions among GC-Tfh clusters. Ligand-receptor pairs were ranked on the basis of the total number of significant *P* values across the cell populations in the 5 clusters (see Fig 1). Heatmap showing total number of interactions between cell types in the decidua data set obtained using CellPhoneDB v3.0, with subsampling.

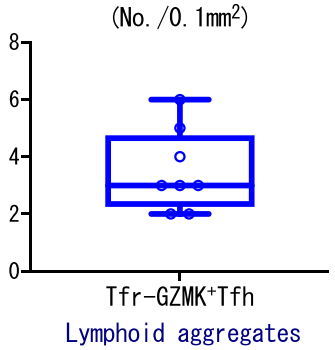

FIG E3. GZMK$^+$ Tfh cells were in physical contact with Tfr cells. A number of GZMK$^+$CD4$^+$CXCR5$^+$ Tfh cells and CD4$^+$CXCR5$^+$Foxp3$^+$ Tfr cells formed close and extensive intercellular plasma membrane contacts. The distance was measured between the edge of each GZMK$^+$CD4$^+$CXCR5$^+$ Tfh-cell nucleus to the edge of the closest GZMK$^+$CD4$^+$CXCR5$^+$ Tfh-cell nucleus, and an internuclear distance of less than 0.4 μm was indicative of a GZMK$^+$ Tfh-Tfr conjugate.

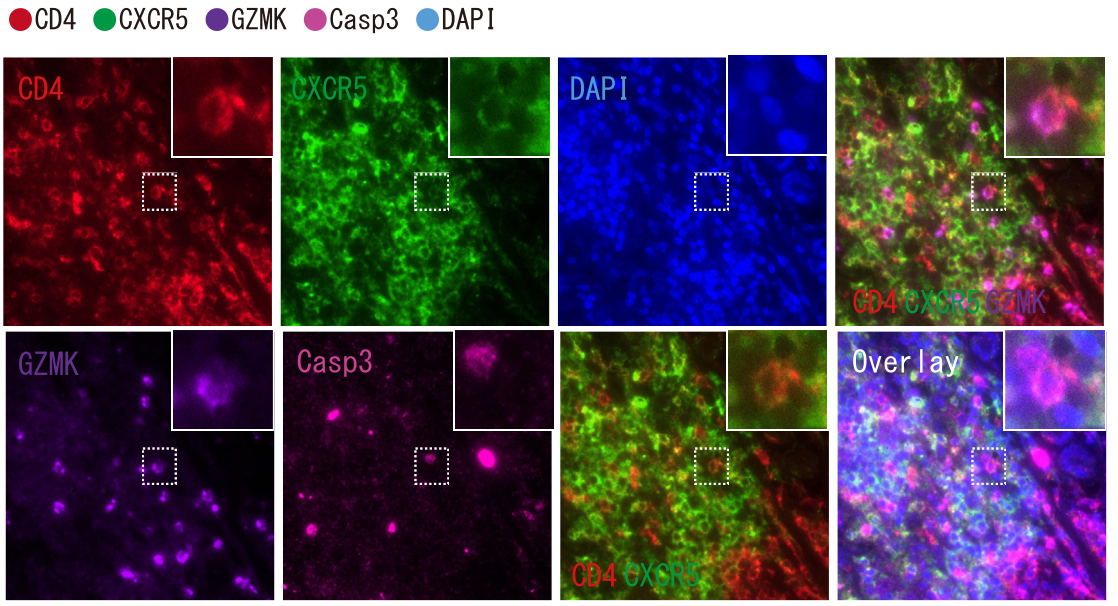

FIG E4. $GZMK^{+}CD4^{+}CXCR5^{+}$ Tfh cells were in physical contact with cleaved caspase 3–expressing cells. Immunofluorescence staining of CD4 (*red*), CXCR5 (*green*), GZMK (*purple*), cleaved caspase 3 (*pink*), and DAPI (*blue*) in affected tissues from a patient with IgG4-RD. *DAPI*, 4′-6-Diamidino-2-phenylindole.

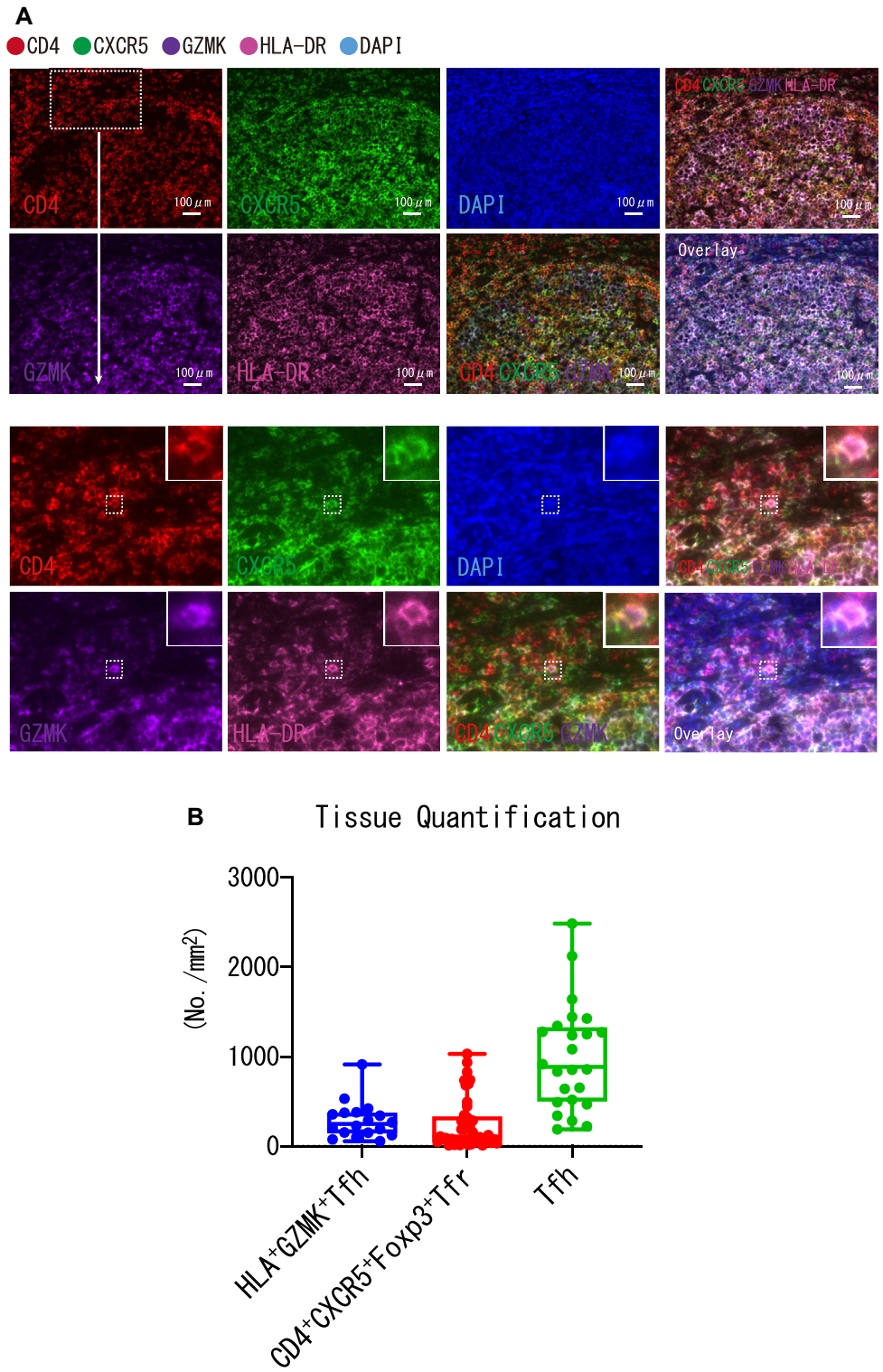

FIG E5. GZMK$^+$HLA$^+$ Tfh cells were detected in affected tissues from patients with IgG4-RD. **A,** Immunofluorescence staining of CD4 (*red*), CXCR5 (*green*), GZMK (*purple*), HLA-DRA (*pink*), and DAPI (*blue*) in affected tissue from a patient with IgG4-RD. **B,** Quantification analysis of CD4$^+$GZMK$^+$HLA$^+$CXCR5$^+$ Tfh cells, CD4$^+$CXCR5$^+$Foxp3$^+$ Tfr cells, and CD4$^+$CXCR5$^+$ Tfh cells by multicolor immunofluorescence of affected SGs from patients with IgG4-RD. *DAPI*, 4′-6-Diamidino-2-phenylindole.

TABLE E1. Background data and clinical and serological findings in 6 patients with IgG4-RD for whom affected SG biopsies were analyzed by scRNA-seq

Background			Clinical findings		Serological findings								Histological findings		Total activity score
Patient no.	Age (y)	Sex	Other swelling lesions	No. of affected organs	SS-A/Ro	SS-B/La	IgG	IgG4	IgE	CRP	RF	ANA	Lymphocytic infiltration (Greenspan histopathologic grade)	IgG4/IgG (%)	Organ/sites (×2 if urgent) + serum IgG4 score
Pt 1	73	M	SMG, LN, PG, AA	4	—	—	1852	708	298	0.04	5	±	3+	84	9
Pt 2	57	M	SMG, LN, PG, PGD, IP	5	—	—	1359	180	460	1.68	16	±	3+	40	6
Pt 3	65	F	SMG	1	—	—	1506	201	ND	0.06	—	320	3+	80	2
Pt 4	62	F	SMG	1	—	—	1821	256	ND	—	—	—	3+	70	2
Pt 5	68	F	SMG, LN	2	—	—	3289	1490	ND	0.62	—	—	3+	65	3
Pt 6	73	F	SMG, BD	2	—	—	2446	1140	ND	0.03	—	40	3+	90	5

AA, Abdominal aorta; *ANA*, antinuclear antibodies; *BD*, bile duct; *CRP,* C-reactive protein; *F*, female; *IP*, interstitial pneumonia; *LN*, lymph node; *M*, male; *ND*, not done; *PG*, parotid gland; *PGD*, pituitary gland; *SS-A/Ro*, Sjogren's syndrome-A/Ribonucleoprotein; *SS-B/La*, Sjogren's syndrome-B/La antigen.

TABLE E2. Background data and clinical and serological findings in 41 patients with IgG4-RD for whom SG biopsies were analyzed by *ex vivo in situ* immunofluorescence

Background			Clinical findings		Serological findings								Histological findings	
Patient no.	Age (y)	Sex	Other swelling lesions	No. of affected organs	SS-A/Ro	SS-B/La	IgG	IgG4	IgE	CRP	RF	ANA	Lymphocytic infiltration (Greenspan histopathologic grade)	IgG4/IgG (CD138)
Pt 7	64	M	SMG, LG, LN, PS	4	—	—	2052	748	645	0.09	22	±	3+	50
Pt 8	66	M	SMG, LG, LN, PL, RF, KN	6	—	—	5674	<1500	349	1.28	8	±	3+	62
Pt 9	77	M	SMG, PC, PG, LN, PL, AA, TG	7	—	—	3498	1910	590	0.8	3	±	3+	70
Pt 10	82	F	SMG	1	—	—	2381	823	ND	ND	ND	160	3+	60
Pt 11	78	M	SMG, PC, LG, LN, PL, BD, RF, KN, AA	9	—	—	4217	524	29	0.55	4	40	3+	50
Pt 12	72	M	SMG, LG	2	—	—	1662	458	603	0.13	ND	±	2+	61
Pt 13	74	M	SMG, LG, LN, PC	4	—	—	2247	835	627	0.03	6	—	2+	80
Pt 14	68	F	SMG, LG, LN, PS	3	—	—	2219	152	713	1.19	4	±	3+	75
Pt 15	72	F	SMG, LG, LN, PC, KN, SP	6	—	—	6758	<1500	13	0.09	8	160	3+	62
Pt 16	65	F	SMG	1	—	—	1614	192	52	0.16	<5	—	3+	60
Pt 17	54	F	SMG, LN, PL	3	—	—	3198	1320	ND	1.62	80	—	3+	60
Pt 18	55	M	SMG	1	—	—	2092	510	ND	0.11	ND	—	3+	70
Pt 19	41	M	SMG	1	—	—	2736	931	770	0.07	ND	—	3+	60
Pt 20	61	M	SMG, LG	2	—	—	4970	773	706	0.05	ND	±	3+	70
Pt 21	67	M	SMG	1	—	—	2619	1130	ND	0.14	5	ND	2+	60
Pt 22	76	M	SMG	1	—	—	1954	793	ND	0.02	ND	ND	3+	70
Pt 23	52	F	SMG, LG	2	—	—	1317	318	20	0.07	7	—	3+	50
Pt 24	76	M	SMG, OM	2	—	—	1620	157	257	0.45	ND	ND	3+	70
Pt 25	44	M	SMG, LG, LN	3	—	—	1366	188	1619	0.05	5	—	3+	90
Pt 26	74	M	SMG	1	—	—	5646	<1500	69	0.38	3	40	3+	80
Pt 27	72	F	LG	1	—	—	1180	163	23	0.04	3	—	3+	90
Pt 28	55	M	SMG, LG, LN, AA	4	—	—	1544	629	ND	0.29	5	40	3+	70
Pt 29	71	M	LN, PL, PC	3	—	—	2481	731	ND	0.44	ND	ND	3+	70
Pt 30	53	F	LN, LG	2	—	—	1363	357	ND	0.16	7	51	3+	50
Pt 31	68	M	SMG, LN, lung	3	—	—	1613	320	ND	0.07	ND	ND	3+	60
Pt 32	61	M	LN, SMG, KN	3	—	—	4970	773	706	ND	ND	—	ND	ND
Pt 33	36	M	LN, KN	2	—	—	2837	963	1702	ND	ND	—	ND	ND
Pt 34	67	M	LN, SMG, KN	3	—	—	2619	1130	ND	ND	5	ND	ND	ND
Pt 35	87	M	LG	1	—	—	1048	200	539	0.02	13	—	3+	80
Pt 36	85	F	LG, KN	2	—	—	3868	913	21	0.07	5	—	3+	70
Pt 37	50	F	LG, SMG	2	—	—	1154	142	301	0.26	7	—	3+	90
Pt 38	37	F	LG, SMG	2	—	—	1044	97	66	0.12	11	—	3+	80
Pt 39	35	M	LG	1	—	—	1534	236	364	0.04	5	40	3+	50
Pt 40	64	M	LG, LN	2	—	—	1271	309	519	0.08	18	—	3+	30
Pt 41	84	F	LG	1	—	—	2319	1275	344	0.05	23	160	3+	80
Pt 42	43	F	LG	1	—	—	1810	551	186	0.24	5	—	3+	90
Pt 43	64	M	LG, LN	2	—	—	1388	253	248	2.16	5	—	3+	60
Pt 44	55	F	LG	1	—	—	1722	294	118	0.12	ND	40	3+	70
Pt 45	61	M	KN, LG, SMG, LN, lung	5	—	—	5184	3460	349	0.17	7	—	3+	ND
Pt 46	40	M	KN, LG, SMG	3	—	—	4849	1500	802	0.78	45	—	3+	ND
Pt 47	72	F	KN	1	—	—	3068	1450	310	0.06	<5	—	3+	ND

AP, Autoimmune pancreatitis; *BD*, bile duct; *DM*, diabetes; *F*, female; *KN*, kidney; *LG*, lacrimal gland; *LN*, lymph node; *M*, male; *ND*, not done; *OM*, orbital muscle; *PC*, pancreas; *PG*, parotid gland;*PL*, pleura; *PS*, prostate; *RF*, retroperitoneal fibrosis; *SP*, spleen; *TG*, thyroid gland.

TABLE E3. Background data and clinical and serological findings in 16 patients with SjS for whom SG biopsies were analyzed by *ex vivo in situ* immunofluorescence

Background			Clinical findings	Serological findings									Histological findings
Patient no.	Age (y)	Sex	History of disorder	SS-A/Ro	SS-B/La	IgG	IgA	IgE	IgM	DNA	RF	ANA	Lymphocytic infiltration (Greenspan histopathologic grade)
Pt 1	72	F	—	240<	—	2038	352	ND	128	<0.5	60	2560<	3+
Pt 2	64	F	OST	193	18	ND	ND	ND	ND	ND	ND	160	2+
Pt 3	65	F	ITP	1200<	61	1983	298	ND	135	10	ND	80	3+
Pt 4	53	F	OST, breast cancer OST	149	—	1614	184	ND	57	ND	25	ND	2+
Pt 5	76	F	HL, ERM, cerebral, aneurysm	240<	320<	ND	ND	ND	ND	ND	ND	ND	2+
Pt 6	55	M	Dysthyreosis, HL, cataract	240<	320<	ND	ND	ND	ND	ND	ND	ND	2+
Pt 7	58	F	Pancytopenia, dysthyreosis, BA	240<	320<	2366	275	ND	320	ND	ND	40	3+
Pt 8	36	F	—	1200<	22	1889	217	ND	163	<10	9	ND	2+
Pt 9	63	F	OST, HT	240<	1	2771	348	ND	70	2	12	160	2+
Pt 10	72	F	AP, DM, fatty liver	240<	60	1564	149	ND	131	ND	ND	40	2+
Pt 11	64	F	—	240<	320<	3166	266	ND	198	1.4	65	ND	3+
Pt 12	65	F	—	240<	1	1380	189	ND	120	1.6	ND	160	2+
Pt 13	53	F	AP, DM, renal angiomyolipoma	240<	140	2607	239	ND	32	ND	ND	2560	2+
Pt 14	76	F	Hepatic cirrhosis	240<	—	ND	ND	ND	ND	ND	ND	ND	2+
Pt 15	36	F	—	240<	—	1984	315	ND	108	5.1	62	320	3+
Pt 16	63	F	—	240<	—	1665	234	423	232	ND	ND	40	3+

AP, Autoimmune pancreatitis; *BA*, bronchial asthma; *DM*, diabetes mellitus; *ERM*, epiretinal membrane; *F*, female; *HL*, hyperlipemia; *HT*, hypertension; *ITP*, idiopathic thrombocytopenic purpura; *M*, male; *ND*, not done; *OST*, osteoporosis.